Environmental Energy and Economic Research 2021 5(4): S020
DOI 10.22097/eeer.2021.281109.1195

Research Article

Exergoeconomic Optimization of a Novel Hydrogen Generation System Based on Geothermal Energy

Ebrahim Aghaie [a], Ehsanolah Assareh [a], Hossein Yousefi [b,*], Rahim Moltames [b], Amirhossein Fathi [c], Kianoosh Choubineh [b]

[a] Dezful Branch, Islamic Azad University, Dezful, Iran
[b] Faculty of New Sciences and Technologies, University of Tehran, Tehran, Iran
[c] School of Mechanical Engineering, Shiraz University, Shiraz, Iran

Received: 25 March 2021 /Accepted: 21 July 2021

Abstract
Hydrogen can be a good energy carrier for renewable energies in the long term due to its appropriate characteristics. However, hydrogen alone is not found in nature and cannot be produced directly. For this purpose, some energy needs to be spent on hydrogen separation. One of the most important hydrogen production methods is the use of electric power to separate hydrogen in an electrolyzer system. In this paper, an exergoeconomic and thermodynamic procedure is applied to the analysis of a novel power generation system based on geothermal energy for hydrogen production. A recuperator is used in the novel system to increase the performance of the system. Five decision variables are considered to optimize system performance. The objective is to maximize the exergy efficiency and on the other hand, minimize the total cost rate of the system. The results of the simulation show that incorporating the recuperator increases the total power production by 20.65%, the energy efficiency by 20.71%, the exergy efficiency by 20.66%, and hydrogen production by 11.91%. Moreover, implementing the particle swarm optimization (PSO) algorithm increases power generation by 4.3%, energy efficiency by 4.2%, exergy efficiency by 4.3%, hydrogen production by 1%, and decreases cost rate by 1%.
Keywords: Hydrogen, organic Rankine cycle, multi-objective optimization, geothermal energy.

Introduction

Energy experts believe that utilizing hydrogen energy systems can be a good solution to the problem of replacing fossil fuels with renewable energies and consequently, reducing pollutant emissions (Midilli and Dincer, 2007; Yilanci, Dincer and Ozturk, 2009). Hydrogen, as a clean energy carrier, can be used in energy systems to eliminate the problem of uncertainty in renewable energy resources which is considered as the most important challenge against boosting these energies through the world. However, pure hydrogen cannot be found in nature and requires a lot of energy to separate it. To overcome this problem, and avoid using fossil fuels, renewable energies can be utilized to produce pure hydrogen (Momirlan and Veziroglu, 2005). Geothermal energy as

* Corresponding author E-mail: Hosseinyousefi@ut.ac.ir

a renewable energy source has great potential in producing hydrogen. The output power produced from the geothermal source can be used for hydrogen production utilizing the water electrolysis process (Yilmaz and Kanoglu, 2014).

Although many studies have been conducted to evaluate the role of solar energy, wind energy, and nuclear energy on hydrogen production, limited studies exist on using geothermal energy. However, we here present some of the relevant studies in the literature. Kanoglu et al. (Kanoglu, Ayanoglu and Abusoglu, 2011) performed an exergoeconomic evaluation within high-temperature steam electrolysis (HTSE) system for three environmental temperatures. According to their results, the capital investment cost, the operating and maintenance costs, and the total cost of the system were determined as 422.2, 2.04, and 424.3 €/kWh, respectively. Ahmadi et al. (Ahmadi, Dincer and Rosen, 2013a) conducted an exergy and exergy analyses of hydrogen production via solar-boosted ocean thermal energy conversion and PEM electrolysis. According to their simulation results, the exergy and energy efficiencies were obtained as 22.7% and 3.6%, respectively. Furthermore, the hydrogen production rate was calculated as 1.2 kg/hr. Esmaili et al. (Esmaili, Dincer and Naterer, 2012) analyzed a novel low-temperature electrolysis hydrogen production system using molybdenum-oxo catalysts in the cathode and a platinum-based anode. They presented the system evaluation results and compared them with those of the previous studies to show the promising performance of the novel system. Kanoglu et al. (Kanoglu, Dincer and Cengel, 2008) proposed three possible cases of using geothermal energy to produce hydrogen using gas liquefaction. Their results showed that precooling the gas in a geothermal absorption cooling system has a significant energy saving potential. Bicer et al. (Bicer and Dincer, 2016) developed a novel hydrogen production system based on solar and geothermal energy. The results of their study showed that the energy and exergy efficiencies of the overall system can reach up to 10.8% and 46.3% respectively for a geothermal water temperature of 210 °C. Yuksel et al. (Yuksel, Ozturk and Dincer, 2018) conducted a thermodynamic assessment of a novel integrated system based on geothermal energy for power, heating, hydrogen, cooling, and hot water purposes. According to their simulation results, the energy and exergy efficiencies were obtained as 42.59% and 48.24%, respectively.

As can be seen from the literature review, limited studies have been done on the exergoeconomic optimization of the hydrogen production system using geothermal energy and (Proton Exchange Membrane (PEM) electrolyzer. Therefore, in this paper, an improved hydrogen production system incorporating geothermal energy and PEM electrolyzer is thermodynamically analyzed and finally optimized using the PSO algorithm. The following sections first introduce the methodology used in this paper, including the mathematical model of the electrolyzer, the mathematical model of energy analysis, the mathematical model of exergy, and thermoeconomic analysis of the system. Next, the optimization model and affecting parameters in the optimization results will be investigated. Then, the results of adding the recuperator and its effect on the system performance are reported. Finally, the results of the parametric analysis, as well as optimization results, are reported and discussed.

Methodology

The detailed layout of the system studied in Ref. (Yilmaz, 2017) is shown in figure 1(a). This system is designed to produce hydrogen using the geothermal energy source and PEM electrolyzer. The high-temperature geothermal fluid first enters the separator and its vapor phase enters the steam turbine to generate power. The remaining is the saturated liquid phase that enters the heat exchanger and delivers its heat to the organic Rankine cycle. The organic fluid is converted to

steam in the heat exchanger and enters the isobutane turbine to generate power. The output power of these two turbines is used to generate hydrogen using the PEM electrolyzer. In the present study, a recuperator is added to the Organic Rankine Cycle (ORC) to increase the cycle performance (See figure 2(b)).

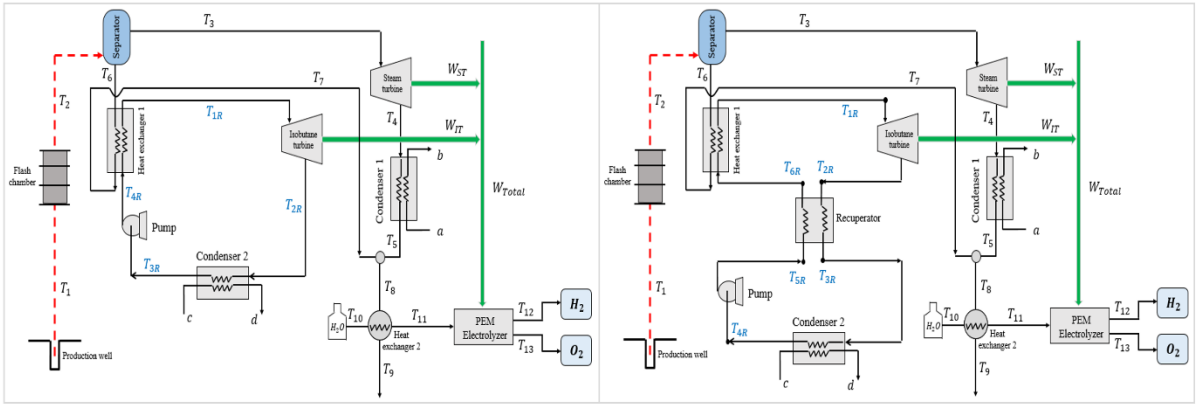

Figure 1. The schematic diagram of the system1 (a) and system2 (b)

The combination of MATLAB and REFPROP software is used to simulate the system. The REFPROP software is a computer-based database consist of the thermodynamic properties of different fluids used in the industry. The PSO algorithm is also used to optimize the system, which will be described in the optimization section.

Electrolyzer

Figure 2 shows a brief schematic of a PEM electrolyzer. The reactions in the anode and cathode of a PEM electrolyzer are written as follows (Shiva Kumar and Himabindu, 2019):

Anode: $$H_2O \rightarrow 2H^+ + \frac{1}{2}O_2 + 2e^-$$

Cathode: $$2H^+ + 2e^- \rightarrow H_2$$

Total reaction: $$H_2O_{(L)} \rightarrow H_{2(g)} + \frac{1}{2}O_{2(g)}$$

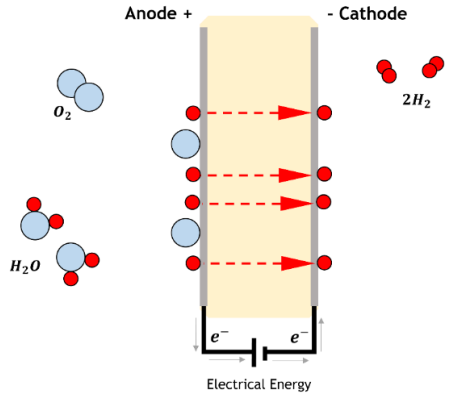

Figure 2. Brief schematic of a PEM electrolyzer single cell

Gibbs free energy is given by (Ahmadi, Dincer and Rosen, 2013b):

$$\Delta G = \Delta H - T\Delta S \quad (1)$$

Where ΔH is the enthalpy change in J/mol, ΔS is the entropy changes in J/mol.K, and T is the temperature in Kelvin. Under ideal conditions, the heat generated during the reaction is continuously excreted from the system, so the system temperature does not change. The reversible potential is calculated using the following equation:

$$V_0 = -\frac{\Delta G}{2F} \quad (2)$$

In the above equation, F is the Faraday constant and is equal to 96485.33 C/mol. The open-circuit voltage for PEM electrolyzer (V_0) is calculated using the Nernst equation:

$$V_0 = 1.229 - 8.5 \times 10^{-3}(T_{PEM} - 298) \quad (3)$$

The voltage of a single cell in PEM electrolyzer (V) is defined as follows:

$$V = V_0 + V_{act.a} + V_{act.c} + V_{ohm} \quad (4)$$

Here, $V_{act,a}$ indicates the activation voltage drop at the anode, $V_{act,c}$ indicates the activation voltage drop at the cathode and V_{ohm} indicates the voltage drop due to ohmic losses. Part of the applied voltage to the PEM electrolyzer is lost due to the transfer of electrons from the electrode surface during the chemical process. The activation energy at both the cathode and anode sides can be expressed by the Volmer-Butler equation:

$$V_{act.i} = \frac{RT}{F} sinh^{-1}\left(\frac{J}{2J_{0.i}}\right) \quad (5)$$

Where $J_{0,i}$ is the anode/cathode current exchange density (A/cm^2) and is given by:

$$J_{0.i} = J_i^{ref} exp\left(-\frac{V_{act.i}}{RT}\right) \quad (6)$$

The ohmic voltage drop (V_{ohm}) occurs due to the electrical resistance of the PEM electrolyzer. This voltage drop varies depending on the type of PEM electrolyzer and the type of electrodes and varies linearly with the current density. The following equation shows the ohmic voltage drop in terms of PEM resistance (R_{PEM}) and current density (J) (Ahmadi, Dincer and Rosen, 2013a), (Ni, Leung and Leung, 2008), (Ebrahimi, Keshavarz and Jamali, 2012):

$$V_{ohm} = JR_{PEM} \quad (7)$$

Where:

$$R_{PEM} = \int_0^D \frac{dx}{\sigma_{mem}[\lambda(x)]} \quad (8)$$

And,

$$\lambda(x) = \frac{\lambda_a - \lambda_c}{D} x + \lambda_C \quad (9)$$

$$\sigma_{mem}[\lambda(x)] = [0.5139\lambda(x) - 0.326]exp\left[1268\left(\frac{1}{303} - \frac{1}{T}\right)\right] \quad (10)$$

Here, D is the membrane thickness, λ_a is the water content at the anode side, and λ_c is the water content at the cathode side.The mass flow rate of hydrogen produced in the electrolyzer system can be expressed as follows (Ratlamwala, Dincer and Gadalla, 2012):

$$\dot{N}_{H_2.out} = \frac{J}{2F} = 2\dot{N}_{H_2O.reacted} \quad (11)$$

The input data used in the PEM electrolyzer simulation are shown in table 1.

Table 1. Input data used for the PEM electrolyzer simulation (Ahmadi, Dincer and Rosen, 2013a), (Ni, Leung and Leung, 2008), (Ahmadi, Dincer and Rosen, 2013b)

Parameter	Description	Value	Unit
P_{O_2}	Oxygen pressure	1.0	*atm*
P_{H_2}	Hydrogen pressure	1.0	*atm*
λ_a	water content at the anode side	14	-
λ_c	water content at the cathode side	10	-
D	membrane thickness	100	μm
J_a^{ref}	the pre-exponential factor for anode	1×10^5	A/m^2
J_c^{ref}	the pre-exponential factor for cathode	10	A/m^2
T_{el}	Electrolyzer temperature	70	*C*

Energy analysis

The conservation of mass and energy laws are used for energy analysis of the system. For this purpose, each component in the system is considered a control volume. For a control volume with input *i* and output *o*, the conservation of mass and energy laws can be written as follows ('Energy and Exergy Efficiency Improvement of a Solar Driven Trigeneration System Using Particle Swarm Optimization Algorithm', 2019):

$$\sum \dot{m}_i = \sum \dot{m}_o \tag{12}$$

$$\sum \dot{Q} - \sum \dot{W} = \sum \dot{m}_o h_o - \sum \dot{m}_i h_i \tag{13}$$

The following assumptions are taken into account in energy analysis:

- ✓ The system is in steady-state pressure drop in pipes, recuperator, condenser, separator, and heat exchangers are ignored.
- ✓ The process inside the valve is considered as isentropic.
- ✓ The processes inside the turbines and pumps are not isentropic. To show this in the mathematical model, Isentropic efficiencies are considered for turbines and pumps.
- ✓ The fluid in the condenser outlet and evaporator outlet is considered as saturated liquid and saturated vapor, respectively.
- ✓ Potential and kinetic energies are not taken into account in energy analysis.

The mass and energy balance equations for different components of the system are given in table 2.

Exergy analysis

Exergy is the maximum available work that can be taken from the energy. Exergy efficiency can be used to evaluate the energy quality and performance of the system (Azizimehr, Assareh and Moltames, 2019). The general equation of exergy by ignoring of effects of nuclear, magnetic, electrical, and surface tension is defined as follows (Borgnakke and Sonntag, no date), (Bejan, Tsatsaronis and Moran, 1996):

$$\psi = (h_{tot} - T_0 s) - \left(h_{tot,0} - T_0 s_0\right) = \left(h - T_0 s + \frac{1}{2}V^2 + gZ\right) - (h_0 - T_0 s_0 + gZ_0) \tag{14}$$

Table 2. Mass and energy balance equations for different components of the system

Component	Equilibrium equations
Separator	$m_2 h_2 = m_6 h_6 + m_3 h_3$ $m_2 = m_6 + m_3$
Steam turbine	$W_{ST} = m_3(h_3 - h_4)$ $m_3 = m_4$
Condenser 1	$m_4(h_4 - h_5) = m_a(h_b - h_a)$ $m_4 = m_5$ $m_a = m_b$
Heat exchanger 1	$m_6(h_6 - h_7) = m_{1R}(h_{1R} - h_{6R})$ $m_6 = m_7$ $m_{1R} = m_{6R}$
Isobutane turbine	$W_{IT} = m_{1R}(h_{1R} - h_{2R})$ $m_{1R} = m_{2R}$
Recuperator	$m_{2R}(h_{2R} - h_{3R}) = m_{6R}(h_{6R} - h_{5R})$ $m_{2R} = m_{3R}$ $m_{5R} = m_{6R}$
Condenser 2	$m_{3R}(h_{3R} - h_{4R}) = m_d(h_d - h_c)$ $m_{3R} = m_{4R}$ $m_c = m_d$
Pump	$W_{Pump} = m_{5R}(h_{5R} - h_{4R})$ $m_{5R} = m_{4R}$
Heat exchanger 2	$m_{10}(h_{11} - h_{10}) = m_8(h_8 - h_9)$ $m_8 = m_9$ $m_{10} = m_{11}$

Here, suffix 0 indicates the death state characteristics (where T=25℃, P=100Pa). V is the velocity, g is the acceleration of gravity, and Z is the distance. The following assumptions are taken into account in exergy analysis of the system:

- ✓ Physical exergies only are considered for flows.
- ✓ Potential and kinetic exergies are neglected due to the Insignificant changes in velocity (Bejan, Tsatsaronis and Moran, 1996).
- ✓ Chemical exergies are neglected.

Exergy equations considering the first and second laws of thermodynamic for each control volume are given by (Elahifar, Assareh and Moltames, 2019), (Azizimehr, Assareh and Moltames, 2019), (Kaviri, Jaafar and Lazim, 2012):

$$\dot{E}_Q + \sum_i \dot{m}_i e_i = \sum_e \dot{m}_e e_e + \dot{E}_W + \dot{E}_D \tag{15}$$

$$\dot{E}_Q = \left(1 - \frac{T_0}{T}\right)\dot{Q} \tag{16}$$

$$\dot{E}_W = \dot{W} \tag{17}$$

$\dot{E}_W$ is the power (work) exergy, $\dot{E}_D$ is the destruction exergy, $\dot{m}$ is the mass flow rate, and $\dot{E}_Q$ is the exergy of heat. Moreover, i and o indicate the input and output streams, respectively. The exergy efficiency also is defined as the ratio of system output exergy to the system input exergy. The destruction exergy, fuel exergy, and product exergy rates for each component of the system are listed in table 3.

Table 3. Destruction exergy, fuel exergy, and product exergy rates for each component

Component	Equilibrium equations
Flash chamber	$Ex_D = m_1(T_0[S_2 - S_1])$ $Ex_f = Ex_1$ $Ex_p = Ex_2$
Separator	$Ex_D = T_0\{(m_3S_3) + (m_6S_6) - (m_2S_2)\}$ $Ex_f = Ex_2$ $Ex_p = Ex_3 + Ex_6$
Steam turbine	$Ex_D = Ex_3 - Ex_4 - W_{ST}$ $Ex_f = Ex_3 - Ex_4$ $Ex_p = W_{ST}$
Condenser 1	$Ex_D = \left(m_4T_0(S_4 - S_5)\right) + \left(m_aT_0(S_b - S_a)\right)$ $Ex_f = Ex_4 - Ex_5$ $Ex_p = Ex_b - Ex_a$
Condenser 2	$Ex_D = \left(m_{orc}T_0(S_{3R} - S_{4R})\right) + \left(m_dT_0(S_d - S_c)\right)$ $Ex_f = Ex_{3R} - Ex_{4R}$ $Ex_p = Ex_d - Ex_c$
Isobutane turbine	$Ex_D = m_{or}\,T_0(S_{2R} - S_{1R})$ $Ex_f = Ex_{1R} - Ex_{2R}$ $Ex_p = W_{IT}$
Pump	$Ex_D = m_{or}\,T_0(S_{5R} - S_{4R})$ $Ex_f = Ex_{4R} - Ex_{5R}$ $Ex_p = W_{Pump}$
Heat exchanger 1	$Ex_D = \left(m_6T_0(S_6 - S_7)\right) + \left(m_{orc}T_0(S_{1R} - S_{6R})\right)$ $Ex_f = Ex_6 - Ex_7$ $Ex_p = Ex_{1R} - Ex_{6R}$
Recuperator	$Ex_D = \left(m_{orc}T_0(S_{6R} - S_{5R})\right) + \left(m_{orc}T_0(S_{2R} - S_{3R})\right)$ $Ex_f = Ex_{6R} - Ex_{5R}$ $Ex_p = Ex_{2R} - Ex_{3R}$
Heat exchanger 2	$Ex_D = \left(m_{12}T_0(S_{17} - S_{12})\right) + \left(m_{15}T_0(S_{15} - S_{16})\right)$ $Ex_f = Ex_{15} - Ex_{16}$ $Ex_p = Ex_{17} - Ex_{12}$

Exergoeconomic analysis

The cost analysis in this paper relies on defining the cost of each component, operating and maintenance (O&M) costs, and the cost of fuel consumption. According to the cost equilibrium model, the sum of output exergy costs of flows is equal to the sum of input exergy costs plus the investment $\left(\dot{Z}_k^{Cl}\right)$, the operation, and maintenance costs $\left(\dot{Z}_k^{OM}\right)$. The cost balance and their auxiliary equations for each component of the system are shown in table 4. For each component based on the heat and power received, it can be written (Boyaghchi and Heidarnejad, 2015):

$$\sum_e \dot{C}_{e,k} + \dot{C}_{W,k} = \dot{C}_{i,k} + \sum_i \dot{C}_{i,k} + \dot{Z}_k^{Cl} + \dot{Z}_k^{OM} \tag{18}$$

$$\dot{Z}_k = \dot{Z}_k^{Cl} + \dot{Z}_k^{OM} \tag{19}$$

$$\dot{C}_i = c_i\dot{X}_i \tag{20}$$

The investment cost of each component is given by the following equations:

Heat exchanger (Mohammadkhani *et al.*, 2014)**:**

$$Z_{HE}^{Cl} = 130\left(\frac{A_{HE}}{0.093}\right)^{0.78} \quad (21)$$

Condenser (Mohammadkhani *et al.*, 2014)**:**

$$Z_{Cond}^{Cl} = 1773\dot{m}_5 \quad (22)$$

Pump (Mohammadkhani *et al.*, 2014)**:**

$$Z_{Pump}^{Cl} = 3540\dot{W}_{Pump}^{0.71} \quad (23)$$

Turbine (El-Emam and Dincer, 2013)**:**

$$log_{10}^{Z_{Turb}^{Cl}} = 2.6259 + 1.4398log_{10}^{(\dot{W}_{Turb})} - 0.1776\left[log_{10}^{(\dot{W}_{Turb})}\right]^2 \quad (24)$$

In the above equations, A_{HE} is the heat exchanger area (m^2), W_{pump} is the pump power consumption (kW), and W_{Turb} is the turbine power production (kW).

The investment cost rate of each component is calculated as follows (Mohammadkhani *et al.*, 2014):

$$\dot{Z}_k = Z_k^{Cl} \times CRF \times {}^{\varphi}/_{t} \quad (25)$$

Where $\dot{Z}_k$ is the investment cost rate of k^{th} system (\$/hour), Z_k^{Cl} is the investment cost of k^{th} system (\$), φ is the maintenance factor (assumed to be 1.06), t is the number of hours per year that the unit operates (t=7446), and CRF is the Capital Recover Factor, which can be expressed as (Garousi Farshi, Mahmoudi and Rosen, 2013):

$$CRF = \frac{i(1+i)^N}{(1+i)^N - 1} \quad (26)$$

Here, i is the discount rate (assumed to be 10%) and n is the system life (assumed to be 20 years).

Table 4. Cost balance and their auxiliary equations for each component of the system

Component	Cost rate balance	Auxiliary equation
Flash chamber	$C_1 + \dot{Z}_{F,ch} = C_2$	-
Steam turbine	$C_2 + \dot{Z}_{ST} = C_3 + C_6$	$\frac{C_3}{Ex_3} = \frac{C_6}{Ex_6}$
	$C_3 + \dot{Z}_{ST} = C_{W,ST} + C_4$	$\frac{C_3}{Ex_3} = \frac{C_4}{Ex_4}$
Condenser 1	$C_a - C_b + \dot{Z}_{cond1} = C_4 - C_5$	$\frac{C_4}{Ex_4} = \frac{C_5}{Ex_5}$
Heat exchanger 1	$C_6 - C_7 + \dot{Z}_{HE1} = C_{1R} - C_{6R}$	$\frac{C_6}{Ex_6} = \frac{C_7}{Ex_7}$
Isobutane turbine	$C_{1R} + \dot{Z}_{IT} = C_{W,IT} + C_{2R}$	$\frac{C_{1R}}{Ex_{1R}} = \frac{C_{2R}}{Ex_{2R}}$
Condenser 2	$C_d - C_c + \dot{Z}_{Cond2} = C_{3R} - C_{4R}$	$\frac{C_{3R}}{Ex_{3R}} = \frac{C_{4R}}{Ex_{4R}}$
Recuperator	$C_{5R} - C_{6R} + \dot{Z}_{rec} = C_{3R} - C_{2R}$	$\frac{C_{2R}}{Ex_{2R}} = \frac{C_{3R}}{Ex_{3R}}$
Pump	$C_4 + C_{W,pump} + \dot{Z}_{pump} = C_{5R}$	-
Heat exchanger 2	$C_8 - C_9 + \dot{Z}_{HE2} = C_{11}$	$\frac{C_8}{Ex_8} = \frac{C_9}{Ex_9}$

Optimization

In the present study, six variables affecting the system performance are taken into account as decision variables in the optimization model. The feasible range for these variables is shown in table 5.

Table 5. The feasible range of decision variables

Decision variable	Feasible range
Isobutane turbine input temperature	$130 \leq T_{1r}(℃) \leq 150$
Flash chamber pressure	$100 \leq P_2\ (kPa) \leq 1000$
Condenser1 outlet pressure	$5 \leq P_5\ (kPa) \leq 15$
Steam turbine isentropic efficiency	$70 \leq \eta_{iso-ST}\ (\%) \leq 90$
Isobutane turbine isentropic efficiency	$70 \leq \eta_{iso-IT}\ (\%) \leq 90$
Pump isentropic efficiency	$70 \leq \eta_{iso-pump}\ (\%) \leq 90$

Energy systems optimization mostly needs to consider several objectives. One of the approaches in multi-objective optimization problems is the weight of objective functions. In this approach, a weight is assigned to each objective function, so that the sum of these terms ($w_1 \times \eta_{ex} + w_2 \times (1 - C_{P.total})$) forms the final objective function (F):

$$Max\ F\left(T_{1r}.P_2.P_5.\eta_{iso-ST}.\eta_{iso-IT}.\eta_{iso-pump}\right) = w_1 \times \eta_{ex} + w_2 \times (1 - C_{P.total}) \quad (27)$$

The constraints on the weights are written as follows:

$$0 \leq w_1.w_2 \leq 1 \quad (28)$$

$$w_1 + w_2 = 1 \quad (29)$$

In the optimization of the present study, the values of w_1 and w_2 are considered as 0.88 and 0.12, respectively. Choosing these values depends on the designer's priorities. Details of the PSO algorithm are provided in Ref. (Keykhah *et al.*, 2019).

Validation

The validation of the present work is done by comparing the results of the simulation of the system without considering the innovation (System 1 and without a recuperator) with those of the Ref. (Yilmaz, 2017) (See table 6). Moreover, the results of the PEM electrolyzer simulation are compared with the experimental data presented in Ref. (Yuksel, Ozturk and Dincer, 2018) (see figure 3). As can be seen from table 6, the simulation results of this paper agree well with the results presented in Ref. (Yilmaz, 2017) which indicates the validity of this paper. The slight difference in the parameter values is also related to the differences in the software library (the different thermodynamic properties of the fluids). Furthermore, the good agreement of the electrolyzer results with the experimental data expresses the reliable modeling of the PEM electrolyzer.

Table 6. Thermodynamic characteristics of different points of system 1 presented in this paper (a) compared to values presented in Ref. (Yilmaz, 2017) (b)

State	T (°C)		P (kPa)		h (kJ/kg)		s (kJ/kgK)	
	a	b	a	b	a	b	a	b
0	25	25	100	100	104.9	104.9	0.3673	0.3672
1	199.9	200	1555	1555	852.3	852.3	2.3306	2.331
2	158.8	158.8	600	600	852.3	852.3	2.3520	2.352
3	158.8	158.8	600	600	2756.1	2756	6.7592	6.759
4	45.79	45.81	10	10	2230	2233	7.0487	7.049
5	5.79	45.81	10	10	191.8	191.8	0.6492	0.6492
6	158.8	158.8	600	600	670.3	670.4	1.9308	1.931
7	76	76	600	600	318.7	318.1	1.0276	1.027
1R	148.81	148.8	2100	2100	801.8	802.7	2.6860	2.689
2R	100.41	100.4	400	400	731.6	732.5	2.7194	2.722
3R	29.57	29.61	400	400	270.2	270.4	1.2424	1.243
4R	30.70	30.59	2100	2100	273.8	274.1	1.2442	1.245

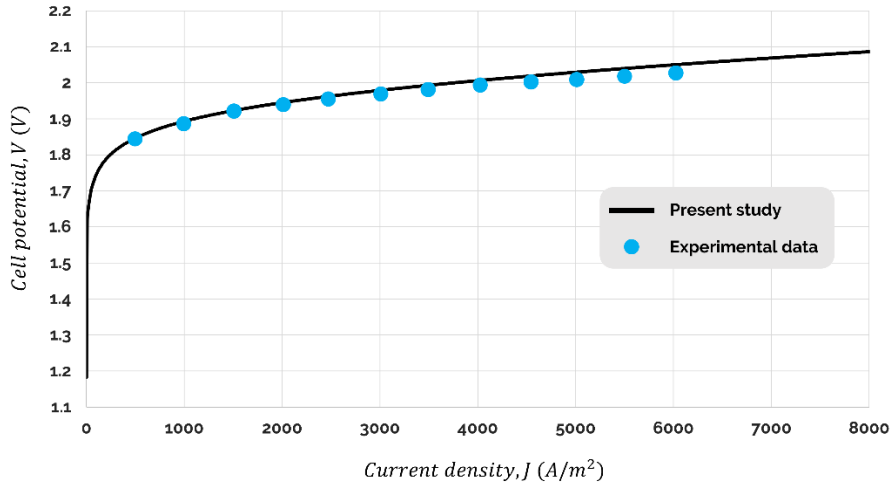

Figure 3. Comparison of the present study with experimental data presented in Ref. (Yuksel, Ozturk and Dincer, 2018)

Results and discussion

System performance

Table 7 shows the values of the performance parameters of the improved system (system 2) compared to the previous system (system 1). As shown in table 7, adding a recuperator to the system significantly improves system performance so that the total output power production is increased by 20.65 %, energy efficiency by 20.71 %, exergy efficiency by 20.66%, and hydrogen production by 11.91%. Table 8 shows the values of the economic parameters for the different components of the system. These parameters include fuel exergy cost rate, product exergy cost rate, exergy destruction rate, and investment cost rate.

Table 7. Performance of system2 (improved and with recuperator) with system 1

Parameter	System 1	System 2	Unit	Improvement (%)
Total power production	6460.3	7794.9	kW	20.65
Energy efficiency	8.64	10.43	%	20.71
Exergy efficiency	39.88	48.12	%	20.66
Hydrogen production rate	18.47	20.67	g/s	11.91

Table 8. Results of the exergoeconomic analysis of the system

Component	$\dot{E}x_F$	$\dot{E}x_P$	$\dot{E}x_D$	$\dot{Z}_k$
Flash chamber	16197	15560	637	0.3334
Separator	15560	15560	0	1.0902
Heat exchanger1	7515.9	7074.8	441.1	0.6948
Heat exchanger2	0.695	0.363	0.332	0.0038
Steam turbine	5315.9	4563.2	752.7	5.9948
Isobutane turbine	7021.5	6148.4	873.1	6.2061
pump	320.45	273.27	47.18	0.3915
Recuperator	1509.5	1439.2	70.3	0.3894
Condenser1	1160.8	237.2	923.6	0.7630
Condenser2	396.9	112.7	284.2	1.5255
PEM electrolyzer	7793.7	6208	1524	143.34

Parametric analysis

In this section, the impact of parameters affecting system performance (decision variables) on objective functions including exergy efficiency and system total cost rate is investigated. Figure 4(a) shows the effect of steam turbine input temperature on exergy efficiency and system total cost rate. As shown in figure 4(a), increasing the steam turbine inlet temperature increases the exergy efficiency of the system and the system cost rate due to an increment in the output power and turbine capacity (which in turn increases the investment cost of the turbine) for constant input exergy. Figure 4(b)shows the effect of the flash chamber pressure on exergy efficiency and system total cost rate. As can be seen from figure 4(b), increasing the flash chamber pressure reduces the exergy efficiency of the system and the total cost rate of the system. Increasing this parameter increases the energy input to the system, which in turn, reduces the efficiency and investment cost of the system. Figure 4(c) shows the effect of the condenser 1 outlet pressure on exergy efficiency and system total cost rate. As illustrated in figure 4(c), increasing the condenser 1 outlet pressure reduces the exergy efficiency of the system and the total cost rate of the system. Increasing this parameter reduces the energy output of the steam turbine, which in turn, reduces the efficiency and investment cost of the system. Figure 4(d) shows the effect of the steam turbine isentropic efficiency on exergy efficiency and system total cost rate. As shown in figure 4(d), increasing steam turbine isentropic efficiency increases the exergy efficiency and the total cost rate of the system. Increasing this parameter increases the output power of the steam turbine, which in turn, increases the efficiency and investment cost of the system. Figure 4(e) shows the effect of the isobutane turbine isentropic efficiency on exergy efficiency and system total cost rate. As shown in figure

4(e), increasing isobutane turbine isentropic efficiency increases the exergy efficiency and the total cost rate of the system. Increasing this parameter increases the output power of the isentropic turbine, which in turn, increases the efficiency and investment cost of the system. Figure 4(f) shows the effect of the pump isentropic efficiency on exergy efficiency and system total cost rate. As illustrated in figure 4(f), increasing pump isentropic efficiency increases the exergy efficiency and the total cost rate of the system. Increasing this parameter reduces the pump consumption, increasing the system output energy, which in turn, increases the efficiency and investment cost of the system. Since the pump power consumption is small compared to the system's total output power, changing pump isentropic efficiency has an insignificant effect on the system efficiency and cost rate.

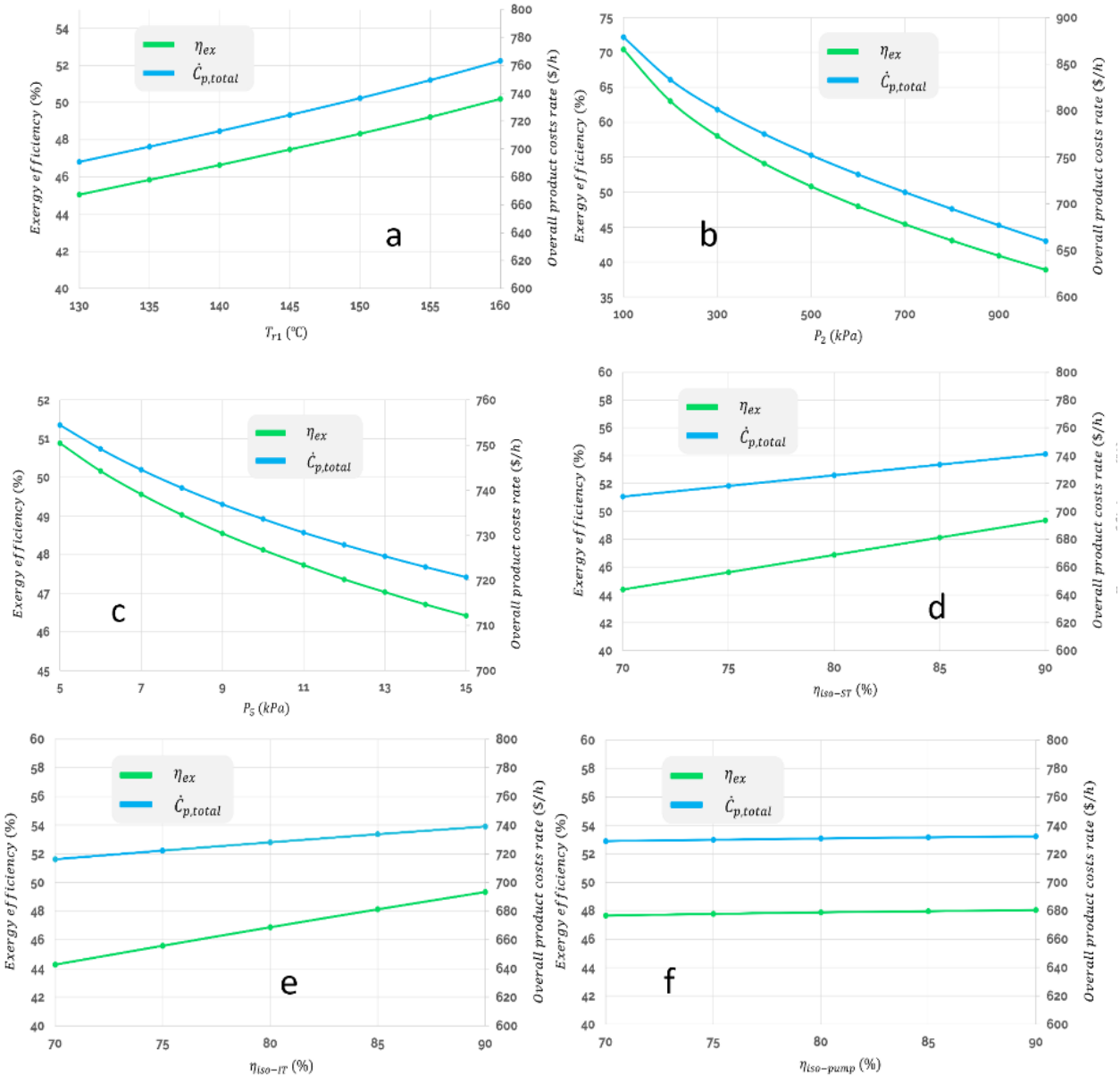

Figure 4. Effects of inputs on exergy efficiency and system total cost rate

Optimization results

Implementing the PSO algorithm has improved the performance of the system. This section follows the results of system optimization. Table 9 shows the results of the multi-objective optimization of the system. According to the table, implementing the optimization algorithm increases the total system power generation from 7794.9 kW to 8129.4 kW. In other words, it increases the system power production by 4.3%. Furthermore, the energy efficiency of the system increased from 10.43% to 10.87%, and the exergy efficiency from 48.12% to 50.19%. On the other hand, multi-objective optimization increases the system hydrogen production from 20.67 g/s to 20.87 g/s. Also, the total cost rate of the system is reduced from 733.62 $/hr to 726.71 $/hr.

Table 9. Optimization results

Parameter		Base case	Optimal case	Improvement (%)
Decision variable	T_{1r} (℃)	148.8	132.84	-
	P_2 (kPa)	600	510	-
	P_5 (kPa)	10	9.8	-
	η_{iso-ST} (%)	85	89	-
	η_{iso-IT} (%)	85	90	-
	$\eta_{iso-pump}$ (%)	85	71	-
Output	W_{total} (kW)	7794.9	8129.4	4.29
	η_{en} (%)	10.43	10.87	4.21
	η_{ex} (%)	48.12	50.19	4.30
	$\dot{m}_{H_2}(g/s)$	20.67	20.87	0.96
	$C_{P-total}$ $(\$/h)$	733.62	726.71	0.94

Conclusion

In the present study, a novel hydrogen generation system based on geothermal energy is investigated and optimized. To increase hydrogen production, a recuperator is used in the novel system. Five parameters that affect the system performance including isobutane turbine input temperature, flash chamber pressure, condenser1 output pressure, steam turbine isotropic efficiency, isobutane turbine isentropic efficiency, and pump isotropic efficiency are considered as decision variables, and their impact on system output is analyzed. The PSO algorithm is used to optimize the system performance. The results of the simulation showed that incorporating the recuperator increases the total power production by 20.65%, the energy efficiency by 20.71%, the exergy efficiency by 20.66%, and hydrogen production by 11.91%. Moreover, implementing the particle swarm optimization (PSO) algorithm increased power generation by 4.3%, energy efficiency by 4.2%, exergy efficiency by 4.3%, hydrogen production by 1%, and decreases cost rate by 1%.

References

Ahmadi, P., Dincer, I., and Rosen, M. A. (2013a). Energy and exergy analyses of hydrogen production via solar-boosted ocean thermal energy conversion and PEM electrolysis. International Journal of Hydrogen

Energy, 38(4), 1795–1805. doi: 10.1016/j.ijhydene.2012.11.025.
Ahmadi, P., Dincer, I., and Rosen, M. A. (2013b). Performance assessment and optimization of a novel integrated multigeneration system for residential buildings. Energy and Buildings, 67, 568–578. doi: 10.1016/j.enbuild.2013.08.046.
Azizimehr, B., Assareh, E., and Moltames, R. (2019). Thermoeconomic analysis and optimization of a solar micro CCHP by using TLBO algorithm for domestic application. Energy Sources, Part A: Recovery, Utilization, and Environmental Effects. doi: 10.1080/15567036.2019.1604883.
Bejan, A., Tsatsaronis, G., and Moran, M. (1996). Thermal Design & Optimization. John Wiley.
Bicer, Y., and, Dincer, I. (2016). Development of a new solar and geothermal based combined system for hydrogen production. Solar Energy, 127, 269–284. doi: 10.1016/j.solener.2016.01.031.
Borgnakke, C., and Sonntag, R. E. (2019). Fundamentals of thermodynamics.
Boyaghchi, F. A., and Heidarnejad, P. (2015). Thermoeconomic assessment and multi objective optimization of a solar micro CCHP based on Organic Rankine Cycle for domestic application. Energy Conversion and Management, 97, 224–234. doi: 10.1016/j.enconman.2015.03.036.
Ebrahimi, M., Keshavarz, A., and Jamali, A. (2012). Energy and exergy analyses of a micro-steam CCHP cycle for a residential building. Energy and Buildings, 45, 202–210. doi: 10.1016/j.enbuild.2011.11.009.
El-Emam, R. S., and Dincer, I. (2013). Exergy and exergoeconomic analyses and optimization of geothermal organic Rankine cycle. Applied Thermal Engineering, 59(1–2), 435–444. doi: 10.1016/j.applthermaleng.2013.06.005.
Elahifar, S., Assareh, E., and Moltames, R. (2019). Exergy analysis and thermodynamic optimisation of a steam power plant-based Rankine cycle system using intelligent optimisation algorithms. Australian Journal of Mechanical Engineering. doi: 10.1080/14484846.2019.1661807.
Energy and Exergy Efficiency Improvement of a Solar Driven Trigeneration System Using Particle Swarm Optimization Algorithm. (2019) Solar Energy Research. doi: 10.22059/JSER.2019.70905.
Esmaili, P., Dincer, I., and Naterer, G. F. (2012). Energy and exergy analyses of electrolytic hydrogen production with molybdenum-oxo catalysts. International Journal of Hydrogen Energy, 37(9), 7365–7372. doi: 10.1016/j.ijhydene.2012.01.076.
Garousi Farshi, L., Mahmoudi, S. M. S., and Rosen, M. A. (2013). Exergoeconomic comparison of double effect and combined ejector-double effect absorption refrigeration systems. Applied Energy, 103, 700–711. doi: 10.1016/j.apenergy.2012.11.022.
Kanoglu, M., Ayanoglu, A., and Abusoglu, A. (2011). Exergoeconomic assessment of a geothermal assisted high temperature steam electrolysis system. Energy, 36(7), 4422–4433. doi: 10.1016/j.energy.2011.03.081.
Kanoglu, M., Dincer, I., and Cengel, Y. A. (2008). Investigation of geothermal energy use in gas liquefaction. Heat Transfer Engineering, 29(10), 885–892. doi: 10.1080/01457630802125781.
Kaviri, A. G., Jaafar, M. N. M., and Lazim, T. M. (2012). Modeling and multi-objective exergy based optimization of a combined cycle power plant using a genetic algorithm. Energy Conversion and Management, 58, 94–103. doi: 10.1016/j.enconman.2012.01.002.
Keykhah, S., Assareh, E., Moltames, R., Izadi, M., and Ali, H. M. (2019). Heat transfer and fluid flow for tube included a porous media: Assessment and Multi-Objective Optimization Using Particle Swarm Optimization (PSO) Algorithm. Physica A: Statistical Mechanics and its Applications. doi: 10.1016/j.physa.2019.123804.
Midilli, A., and Dincer, I. (2007). Key strategies of hydrogen energy systems for sustainability. International Journal of Hydrogen Energy, 32(5), 511–524. doi: 10.1016/j.ijhydene.2006.06.050.
Mohammadkhani, F., Shokati, N., Mahmoudi, S. M. S., Yari, M., and Rosen, M. A. (2014). Exergoeconomic assessment and parametric study of a Gas Turbine-Modular Helium Reactor combined with two Organic Rankine Cycles. Energy, 65, 533–543. doi: 10.1016/j.energy.2013.11.002.
Momirlan, M., and Veziroglu, T. N. (2005). The properties of hydrogen as fuel tomorrow in sustainable energy system for a cleaner planet. International Journal of Hydrogen Energy, 30(7), 795–802. doi: 10.1016/j.ijhydene.2004.10.011.
Ni, M., Leung, M. K. H., and Leung, D. Y. C. (2008). Energy and exergy analysis of hydrogen production

by a proton exchange membrane (PEM) electrolyzer plant. Energy Conversion and Management, 49(10), 2748–2756. doi: 10.1016/j.enconman.2008.03.018.

Ratlamwala, T. A. H., Dincer, I., and Gadalla, M. A. (2012). Thermodynamic analysis of an integrated geothermal based quadruple effect absorption system for multigenerational purposes. Thermochimica Acta, 535, 27–35. doi: 10.1016/j.tca.2012.02.008.

Shiva Kumar, S., and Himabindu, V. (2019). Hydrogen production by PEM water electrolysis – A review. Materials Science for Energy Technologies, 2(3), 442–454. doi: 10.1016/j.mset.2019.03.002.

Yilanci, A., Dincer, I., and Ozturk, H. K. (2009). A review on solar-hydrogen/fuel cell hybrid energy systems for stationary applications. Progress in Energy and Combustion Science, 231–244. doi: 10.1016/j.pecs.2008.07.004.

Yilmaz, C. (2017). Thermoeconomic modeling and optimization of a hydrogen production system using geothermal energy', Geothermics, 65, 32–43. doi: 10.1016/j.geothermics.2016.08.008.

Yilmaz, C., and Kanoglu, M. (2014). Thermodynamic evaluation of geothermal energy powered hydrogen production by PEM water electrolysis. Energy, 69, 592–602. doi: 10.1016/j.energy.2014.03.054.

Yuksel, Y. E., Ozturk, M., and Dincer, I. (2018). Thermodynamic analysis and assessment of a novel integrated geothermal energy-based system for hydrogen production and storage. International Journal of Hydrogen Energy, 43(9), 4233–4243. doi: 10.1016/j.ijhydene.2017.08.137.